Homology Modeling of the Structure of Bacterial Acetohydroxy Acid Synthase and Examination of the Active Site by Site-Directed Mutagenesis †

ARTICLE *in* BIOCHEMISTRY · DECEMBER 1996

Impact Factor: 3.02 · DOI: 10.1021/bi961588i · Source: PubMed

Homology Modeling of the Structure of Bacterial Acetohydroxy Acid Synthase and Examination of the Active Site by Site-Directed Mutagenesis†

Muhammad Ibdah,‡ Ahuva Bar-Ilan,‡ Oded Livnah,§,|| John V. Schloss,⊥ Ze'ev Barak,‡ and David M. Chipman*,‡

Department of Life Sciences, Ben-Gurion University of the Negev, P.O. Box 653, Beer-Sheva 84105, Israel, Department of Structural Biology, Weizmann Institute of Science, Rehovoth, Israel, and Department of Medicinal Chemistry, 4070 Malott Hall, University of Kansas, Lawrence, Kansas 66045

Received July 1, 1996; Revised Manuscript Received October 15, 1996⊗

ABSTRACT: Acetohydroxy acid synthase (AHAS, EC 4.1.3.18) catalyzes the thiamin pyrophosphate (TPP)-dependent decarboxylation of pyruvate and condensation of the resulting two-carbon moiety with a second α-keto acid. It belongs to a family of homologous, TPP-dependent enzymes which catalyze different reactions which start from decarboxylation of α-keto acids. A model for the structure of *Escherichia coli* AHAS isozyme II, based on its homology with pyruvate oxidase and experimental testing of the model by site-directed mutagenesis, has been used here to study how AHAS controls the chemical fate of a decarboxylated keto acid. Because of the potential conformational freedom of the reacting substrates, residues interacting with the substrate could not be identified directly from the model of AHAS. Three residues were considered as candidates for involvement in the recognition of α-ketobutyrate, as the amino acids at these sites in a unique low-specificity AHAS are different from those in typical AHASs, which are highly specific for reaction with α-ketobutyrate as second substrate, in preference to pyruvate. These residues were altered in AHAS II by site-directed mutagenesis. Replacement of Trp464 lowers the specificity by at least 1 order of magnitude, with minor effects on the activity or stability of the enzyme, suggesting that Trp464 contributes ≥ 1.3 kcal mol^{-1} to interaction with the "extra" methyl of α-ketobutyrate. Mutations of Met460 or Thr70 have small effects on specificity and do affect other properties of the protein. A model for enzyme−substrate interactions can be proposed on the basis of these results. The model of AHAS also explains previously reported spontaneous mutants of AHAS resistant to sulfonylurea herbicides, which probably bind in the narrow depression which provides access to the bound TPP. A role for the C terminus of the enzyme polypeptide in determination of the reaction pathway is also possible.

Acetohydroxy acid synthase (AHAS,[1] EC 4.1.3.18, also called acetolactate synthase) belongs to a family of homologous (Green, 1989) thiamin pyrophosphate (TPP)-dependent enzymes, which catalyze processes in which the common first step is decarboxylation of pyruvate (or a similar α-keto acid). The enzymes of this family differ widely, however, with regard to the fate of the TPP-bound "active aldehyde" intermediate formed by the decarboxylation. AHAS catalyzes the condensation of the (hydroxyethyl)thiamin pyrophosphate (hydroxyethyl-TPP) carbanion intermediate with a second α-keto acid to form either of two possible alternative physiologically significant acetohydroxy acid products (Figure 1) (Umbarger, 1987). Pyruvate decarboxylases (and enzymes with related activities) allow protonation of the intermediate, and their products are the respective aldehydes. Pyruvate oxidases catalyze the oxidation of the hydroxyethyl-TPP carbanion to acetyl-TPP, mediated via a tightly bound FAD moiety, and transfer the acetyl group to water or phosphate. While the chemical properties of thiamin pyrophosphate which enable it to participate in the decarboxylation of α-keto acids have been understood for many years (Breslow, 1958; Kluger, 1987), little is known about the role of the enzyme active sites in determining the fate of the hydroxyalkyl-TPP carbanions.

The high-resolution crystallographic structure of pyruvate oxidase from *Lactobacillus plantarum* (LpPOX), determined by Schulz and co-workers (Muller & Schulz, 1993; Muller et al., 1994), has made it possible to begin to understand the mechanisms of the enzymes homologous to it. AHASs have about 26−30% sequence identity with pyruvate oxidases, and it has been suggested that the evolutionary descent of AHASs from a primordial pyruvate oxidase explains the requirement for FAD in these nonoxidative enzymes (Chang & Cronan, 1988; Schloss et al., 1988). These enzymes also share common cofactors (TPP, FAD, and Mg^{2+}) and a common first enzymatic step so that it seems very reasonable to assume that AHASs and LpPOX have structurally homologous active sites. On the basis of this assumption, we have used the crystallographic structure of LpPOX to construct a partial three-dimensional model of AHAS isozyme II from *Escherichia coli* and present this model here.

† This research was partially supported by Grant 93-233 from the United States-Israel Binational Science Foundation (BSF), Jerusalem, Israel, to D.M.C., Z.B., and J.V.S.

* To whom correspondence should be addressed.

‡ Ben-Gurion University of the Negev.

§ Weizmann Institute of Science.

|| Current address: Department of Molecular Biology, Scripps Institute, La Jolla, CA.

⊥ University of Kansas.

⊗ Abstract published in *Advance ACS Abstracts,* November 15, 1996.

[1] Abbreviations: AHAS, acetohydroxy acid synthase; SMM, sulfometuron methyl; LpPOX, pyruvate oxidase from *Lactobacillus plantarum*.

S0006-2960(96)01588-7 CCC: $12.00

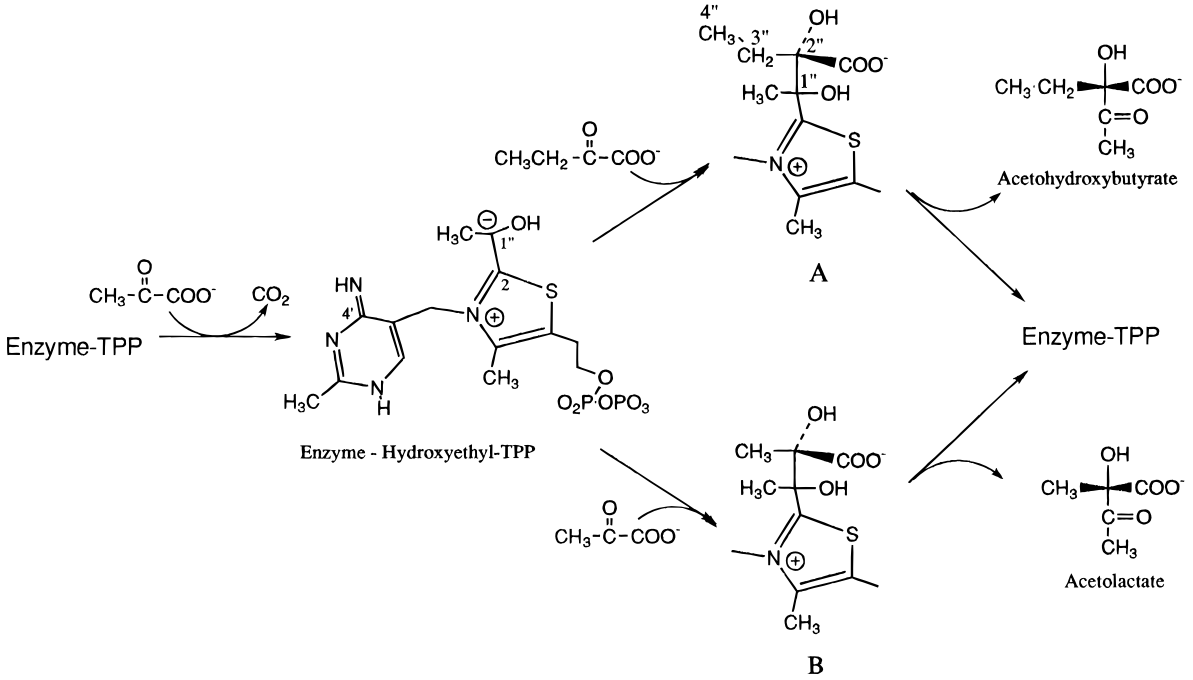

FIGURE 1: Reactions catalyzed by AHAS. The configuration at C1″ of the presumed intermediates A and B (adducts of TPP to one of the alternative acetohydroxy acid products) is not known.

The formation of intermediates covalently attached to the tightly bound (Muller & Schulz, 1993; Muller et al., 1994) coenzyme (*e.g.*, A or B in Figure 1) makes it easy to identify the general region of substrate and product binding in the AHAS model. However, as these intermediates have considerable freedom of rotation about single bonds, the identity of enzyme groups interacting with the substrates still cannot be determined from a homology model alone. The existence of competing reactions catalyzed by AHAS makes it possible to design experiments which can help to identify active site residues which interact with substrates. The hydroxyethyl-TPP intermediate on AHAS (Figure 1) can react with pyruvate, to produce α-acetolactate (a precursor of valine), while when the second acid is α-ketobutyrate, the product is 2-aceto-2-hydroxybutyrate (precursor of isoleucine) (Umbarger, 1987). The ability of most AHASs to favor α-ketobutyrate over pyruvate as the second substrate, by nearly 2 orders of magnitude (Gollop et al., 1989), is of physiological importance (Barak et al., 1987; Gollop et al., 1990). This high selectivity of the enzyme is an interesting example of the general phenomenon of substrate recognition and enzymatic reaction specificity. By considering the specificity properties and amino acid sequences of a number of different AHASs, in the light of the homology model of AHAS II, we were able to propose a model for the substrate recognition site and test it by site-directed mutagenesis. The results of these mutagenesis experiments are reported here.

The experimental identification of substrate specificity determinants reported here also allows us to suggest a general picture for the roles of residues in or near the active site and to consider a wide variety of questions concerning the structure and function of AHASs and related enzymes.

MATERIALS AND METHODS

Homology Modeling of the Protein Structure. In order to build a model of AHAS, the amino acid sequence of the AHAS II catalytic subunit (*ilvG* product) was first aligned with that of LpPOX. Sequences of a number of AHAS catalytic subunits were obtained from the EMBL and GenBank data bases and aligned over their entire length using the program PILEUP from the GCG package (Genetics Computer Group, 1991) with default parameters for peptide alignment. The alignment was adjusted manually and the model then built using the programs FRODO (Jones, 1978) and O (Jones et al., 1991).

Structural illustrations were created from coordinate files with the program MOLSCRIPT (Kraulis, 1991)

Site-Directed Mutagenesis. Mutagenesis of AHAS II was carried out by ligation of a cassette fragment containing the mutation(s) into the plasmid pTG (Yadav et al., 1986), which carries the complete expressible *ilvGM* genes behind the native promoter. All manipulations of the DNA were carried out by standard techniques (Sambrook et al., 1989). For example, to introduce mutations at W464, a 1192-base pair fragment (from the *Eco*RI to *Sph*I sites of pTG) was prepared by the method of splicing by overlap extension (Ho et al., 1989) using as the overlapping internal primers TGGTTCGACAATGGCAGCAACTGT and ACAGTTGCTGCCATTGTCGAACCA, with the bases of the wild-type codons (those underlined) appropriately altered in the construction of mutants. For mutations at M460, the fragment was prepared using ACGGTTAGGGATGGTTCGACAATG and CATTGTCGAACCATCCCTAACCGT as internal primers, with the underlined bases changed. The amplified 1192 bp fragment prepared in this way was isolated and cleaved with *Kpn*I and *Mlu*I to yield a 505 bp fragment, which was ligated into the similarly cleaved pTG. The plasmids were transformed into the AHAS$^-$ *E. coli* K12 strain BUM1, and clones were selected. The sequence within the 500 bp PCR-derived stretch was verified for the plasmids characterized for activity.

Bacterial Strains and Growth. The host strain BUM1 was an AHAS$^-$ *E. coli* K12 strain of genotype *ilvB2102 ilvIH2202* Δ*recA rbs-221 ara thi* Δ(*pro-lac*). It was derived

from CU9090 [originally CU1126 in Harms et al. (1985)] by P1 transduction to introduce the deletion in *recA* (Cohen-Fix & Livneh, 1992). The plasmid was transduced into BUM1 and grown under standard conditions for the expression of AHAS activity (Sella et al., 1993).

The catalytic activity of wild-type and mutant AHASs was determined by the standard colorimetric method (Sella et al., 1993) at 37 °C and pH 7.6 in 0.1 M potassium phosphate buffer containing 40 mM pyruvate, 0.1 mM TPP, 25 μM FAD, and 10 mM $MgCl_2$, unless otherwise indicated. We have shown that many of the properties of AHASs expressed from plasmids in *E. coli* can be reliably determined in bacterial extracts (Barak et al., 1987, and unpublished results), since they involve the dependence of relative activity on concentrations of other factors. Although we expect the relative amounts of protein in extracts from the same host bearing closely related plasmids to be roughly comparable and have confirmed this in a few cases by using semiquantitative immunoblotting techniques (Sella et al., 1993), we can only approximately estimate relative specific activities.

K_M for pyruvate, TPP, or FAD was determined by variation of the concentration of the factor in question, and the results were fit to the Michaelis−Menten equation by a nonlinear least-squares method using ENZFIT. The specificity ratio *R* was determined in direct competition experiments, in which the simultaneous formation of acetohydroxybutyrate and acetolactate is followed in the presence of various concentrations of α-ketobutyrate and 40 mM pyruvate by the gas chromatographic method previously described (Gollop et al., 1989). This determination of *R* does not involve separate kinetic determinations of rates.

The apparent K_i for the herbicide sulfometuron methyl (SMM) was estimated from the average rate over 20 min in the presence of varied concentrations of SMM and 40 mM pyruvate. When 20 μM SMM led to a less than 10% decrease in activity by this method, K_i is >20 μM.

The half-life for loss of activity at 55 °C was estimated by preincubation of the enzyme for varied times in buffer containing 0.1 mM FAD, 1 mM DTT, and 10 mM EDTA, followed by assay for catalytic activity. The loss of activity was approximately pseudo-first-order.

RESULTS AND DISCUSSION

Model of the AHAS II Catalytic Dimer. The catalytic polypeptide of AHAS II has about 27% amino acid sequence identity and 53% sequence similarity (Genetics Computer Group, 1991) to *L. plantarum* pyruvate oxidase (LpPOX). An Eisenberg three-dimensional-compatibility search (Bowie et al., 1991) with the sequence of the AHAS II catalytic subunit, against the protein domain structure data base, gave the highest *Z* scores (15.0−11.2 standard deviations) for separate structural domains of the LpPOX structure, with the next highest *Z* score (9.5) for a domain of the related pyruvate decarboxylase (Arjunan et al., 1996), and no other domains with scores better than 5.5. This, together with a *Z* score of 27.9 for the complete LpPOX structure, implies that it is highly likely that the AHAS II polypeptide is folded in the same general manner as is LpPOX (Bowie et al., 1991).

Each of the enterobacterial AHAS isozymes is composed of a pair of catalytic subunits of about 60 kDa and two smaller, regulatory subunits (Eoyang & Silverman, 1986; Lu & Umbarger, 1987; Squires et al., 1983; Weinstock et al., 1992). The catalytic subunits of AHASs have conserved sequences, with about 40% sequence identity between any two isozymes; the regulatory subunits are far more diverse in size and sequence. We have shown that, at least for some of these enzymes, the large subunits contain all the catalytic machinery required for AHAS activity (Weinstock et al., 1992). Dimerization of the catalytic subunits seems to be required for activity (Vyazmensky et al., 1996). *L. plantarum* pyruvate oxidase (LpPOX), on the other hand, is a tetramer of identical polypeptides 602 amino acids in length. LpPOX has D_2 symmetry and can be considered to be functionally composed of a pair of dimers (Muller & Schulz, 1993). Two equivalent active sites, with one TPP, Mg^{2+} ion, and FAD in each, are formed at the tight interface between the two monomers in each dimer, while the dimer−dimer interfaces have fewer intersubunit contacts (Muller et al., 1994). We assume that a dimer of AHAS catalytic subunits is the minimal structure of functional interest and that a catalytic dimer of LpPOX should be a good model for its three-dimensional arrangement.

The assumption that the interactions within a catalytic dimer are conserved within this family of homologous proteins is supported by the striking similarity in the structures of such dimers in LpPOX and in yeast pyruvate decarboxylase (Arjunan et al., 1996; Muller et al., 1993), as well as in benzoylformate decarboxylase from *Pseudomonas putida* (M. S. Hasson, personal communication). The Mg^{2+}−Mg^{2+} distances in these dimers are quite similar (within 1 Å). On the other hand, we chose to base our model exclusively on the LpPOX structure (rather than on a superposition of all known three-dimensional structures in the homologous family) because of the much greater sequence homology of the AHASs with LpPOX than with any decarboxylase and because of the importance of bound FAD to the structures of both these proteins (Muller et al., 1994; Vyazmensky et al., 1996).

A model of a catalytic dimer of AHAS isozyme II was constructed by standard techniques, starting from an alignment of the sequences of LpPOX and a number of AHAS catalytic polypeptides. The alignment was adjusted to take into consideration the secondary structure elements of LpPOX as well as sequence homologies, and the final alignment used is shown in Figure 2. Sections of the polypeptide chain involving insertions/deletions in AHAS relative to the LpPOX (in general, loop or turn regions) were modeled by choosing appropriate fragments from a Cα library (Jones et al., 1991) and the chains regularized in these regions. Side chains in LpPOX were replaced with those in the homologous positions in the AHAS II sequence and assigned reasonable conformations which avoided steric clashes. A dimer was modeled by assuming the two subunits to be related by the same symmetry transform which relates one monomer to another in a catalytic dimer in LpPOX. The cofactors TPP, Mg^{2+}, and FAD were inserted in the AHAS model in the same positions they occupy in LpPOX. Side chain conformations in a sphere around the TPP were subjected to a round of energy minimization using the InsightII/Discover software from BIOSYM Technologies.

The overall structure of our current model of the AHAS II catalytic dimer is shown in Figure 3. The model appears to be reasonable; it contains few unusual residue conformations and no unacceptable close contacts. The spatial

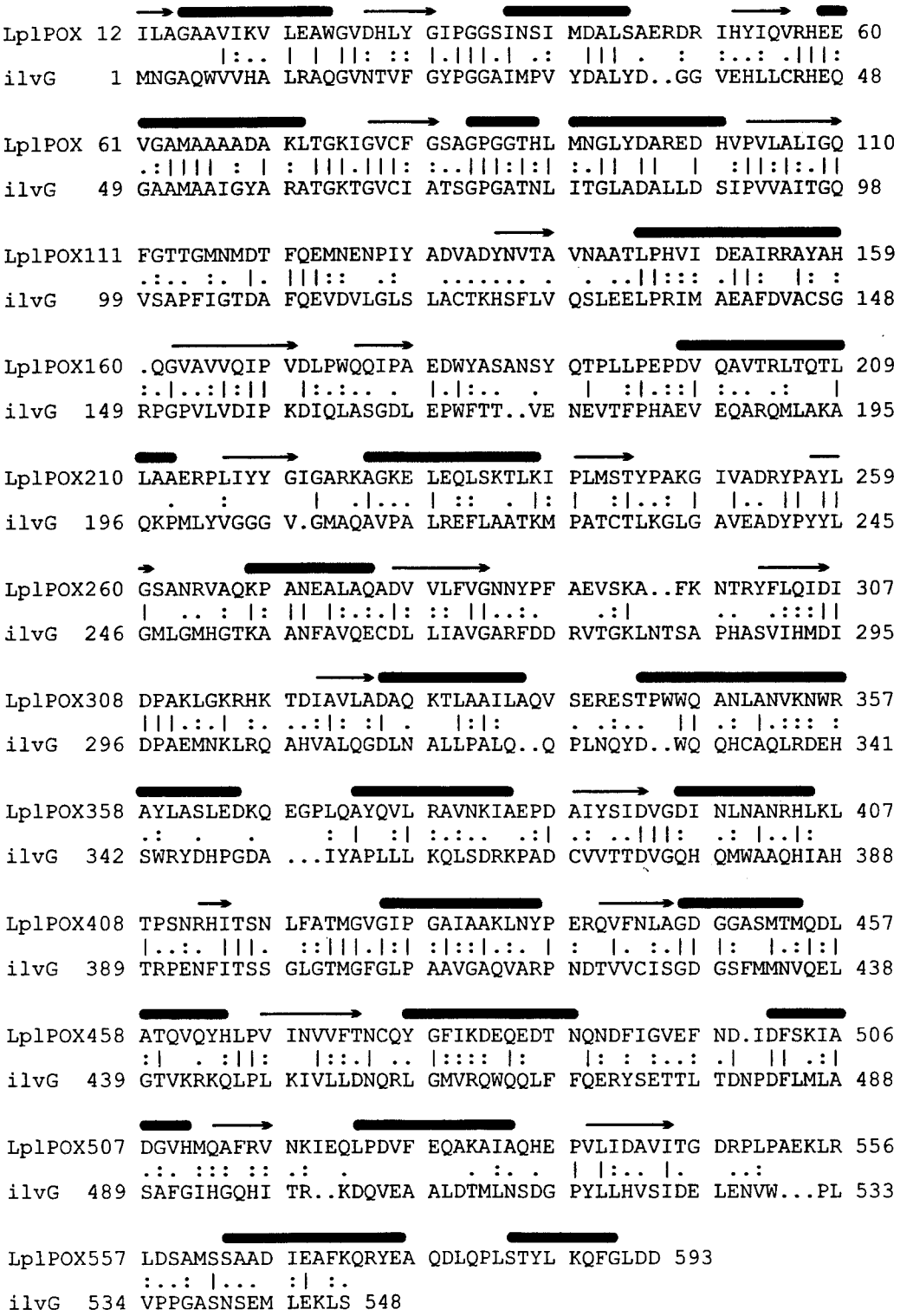

FIGURE 2: Sequence alignment of LpPOX and the catalytic polypeptide of AHAS II used in construction of the model. Secondary structural elements of LpPOX are shown above the sequence (arrows are β-strands and thick bars α-helices). The first nine and last nine residues of LpPOX were not observable in the crystallographic structure (Muller & Schulz, 1993; Muller et al., 1994).

arrangement of the functionally important groups, such as those involved in the Mg^{2+}−pyrophosphate binding region critical to TPP binding (Muller et al., 1993), is maintained. The regions of the AHAS II structure of greatest uncertainty are those which involve deletions/insertions relative to LpPOX so that the main chain conformations chosen are somewhat arbitrary (although not unreasonable). These regions are identified as thin black coils in Figure 3; it can be seen that none is at the dimer interface or in the active site. One such ambiguous region is the long stretch of irregular extended conformation connecting the N-terminal and FAD-binding domains (residues 167−183), which seems exposed and not arranged in a particularly stable manner in the model. In LpPOX, the equivalent region forms part of the interface between dimers in the tetrameric protein. This suggests the possibility that this stretch in AHAS interacts with the small, regulatory subunit; the properties of bacterial AHASs suggest that interaction with the small subunits is required for the formation of stable and active catalytic dimers (Vyazmensky et al., 1996; Weinstock et al., 1992).

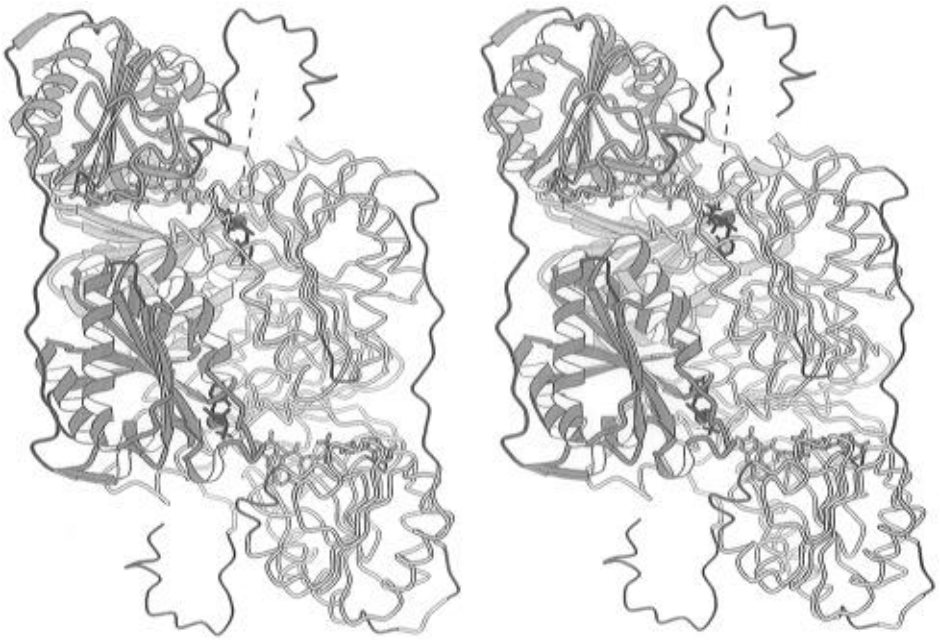

FIGURE 3: Schematic diagram of the model of the AHAS II catalytic dimer. The view is down the 2-fold rotational axis which relates the identical subunits (with the surface homologous to the dimer−dimer interface of LpPOX facing the viewer). Polypeptide A is shown in ribbon diagram form, shaded to indicate the three folding domains: "N-terminal" (closest to the viewer and in dark gray), "FAD-binding" (at top left and intermediate in shading), and "C-terminal" (away from the viewer and light gray). Polypeptide B is shown as an unshaded "worm". Regions where the backbone conformation has the greatest uncertainty, because of deletions/insertions relative to LpPOX, are shown as thinner, black coils. The active sites are formed by the interfaces between the C-terminal domain of one subunit and the N-terminal domain of another and are defined by the bound cofactors TPP (black ball-and-stick structures) and Mg^{2+} (dark spheres). Bound FAD (gray) is also shown. Access of substrates to the active site would be via the narrow channels opening upward and downward in this diagram; a dashed line defines one possible path to the TPP bound between the C-terminal domain of polypeptide A and the N-terminal domain of polypeptide B (see Figure 8). The "tails" extending away from the protein at the C-terminal ends of the subunits are shown in an arbitrary conformation which is unlikely to be stable (see Discussion).

Our model must thus remain incomplete in this region for now. The ambiguous 18-amino acid carboxy-terminal segment of the protein is also of special interest; it is discussed in detail below. Further energy minimization of the model, given these ambiguities, would not be helpful.

Despite these reservations, we suggest that the present model for AHAS II is relevant, both in its general structure and in the nature of the active site (see below), to the FAD-dependent, biosynthetic AHASs in general. For example, an examination of the alignment of the sequences of *all* known AHAS catalytic polypeptides shows that the regions of sequence conservation correspond closely to the domain structure in the model (Figure 4). The sequences of polypeptide segments in the active site in the AHAS II model are strongly conserved in all the AHASs. Details of the active site are discussed below.

Active Site. TPP lies at the bottom of a rather narrow channel at an intersubunit interface in the AHAS model, as it does in the structure of LpPOX on which it is based. Figure 5 shows the thiamin pyrophosphate and the residues around it in the model. There are many polar interactions of the protein with the Mg^{2+}−pyrophosphate and the pyrimidine moieties of the cofactor, homologous with those in the related enzymes (Arjunan et al., 1996; Muller et al., 1993). The thiazolium ring is in a more hydrophobic environment, with the C2 atom exposed in the channel. This model does not lead directly to identification of catalytically important residues of the protein or of the substrate recognition site of AHAS, since the position of, *e.g.*, the "additional" methyl group of acetohydroxybutyrate in intermediate A (Figure 1) relative to the coenzyme is determined by the unknown configuration at C1″ and rotation about three single bonds.

In order to clarify the orientation of the substrate in the active site, we turned to site-directed mutagenesis. The amino acids which were candidates for mutation were chosen by considering the correlation between the specificity properties of several AHASs and the amino acids occupying putative homologous positions in their active sites. An interesting and physiologically significant property of most AHASs is their selectivity in favor of the reaction with α-ketobutyrate (Figure 1). The selectivity in favor of the substrate α-ketobutyrate, with one additional methyl group, is in some cases greater than 60-fold and can be defined by a specificity ratio:

$$R = \frac{V_{AHB}/V_{AL}}{[\alpha\text{-ketobutyrate}]/[\text{pyruvate}]}$$

The specificity R is determined by product analysis in direct competition experiments over a range of α-ketobutyrate and/or pyruvate concentrations and is quite independent of experimental conditions (Barak et al., 1987; Gollop et al., 1989). However, one of the isozymes of enterobacterial AHASs, AHAS I, has a uniquely low selectivity for α-ketobutyrate; $R = 2.0$ (Barak et al., 1987; Gollop et al., 1989, 1990). We asked whether this isozyme has any uniquely different amino acids in the active site, at positions which are conserved in all other AHASs. Figure 6 presents the relevant portions of an alignment of the sequences of LpPOX, AHASs, and several other members of the homologous family. The amino acids at positions 83, 476, and 480 in AHAS I—Cys, Leu, and Gln, respectively—are different from those at the equivalent positions—Thr, Met, and Trp—in *all* other AHASs in the sequence data bases. Amino acids

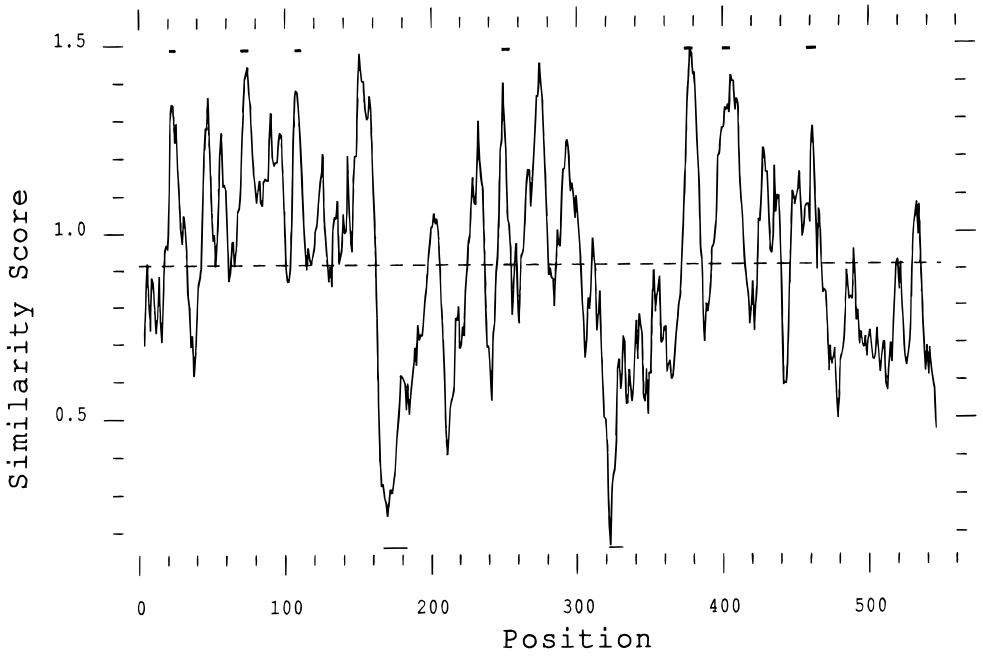

FIGURE 4: Similarity plot for AHAS catalytic sequences. The similarity scores (Genetics Computer Group, 1991) (based on the Dayhoff PAM250 scoring matrix) over a window of six residues for 24 AHAS sequences are plotted against AHAS II sequence position. The two interdomain loops in the AHAS II model are indicated by the lines below the plot. The bars above the plot indicate the segments near the substrate site (see Figure 5) whose sequences are compared in Figure 6.

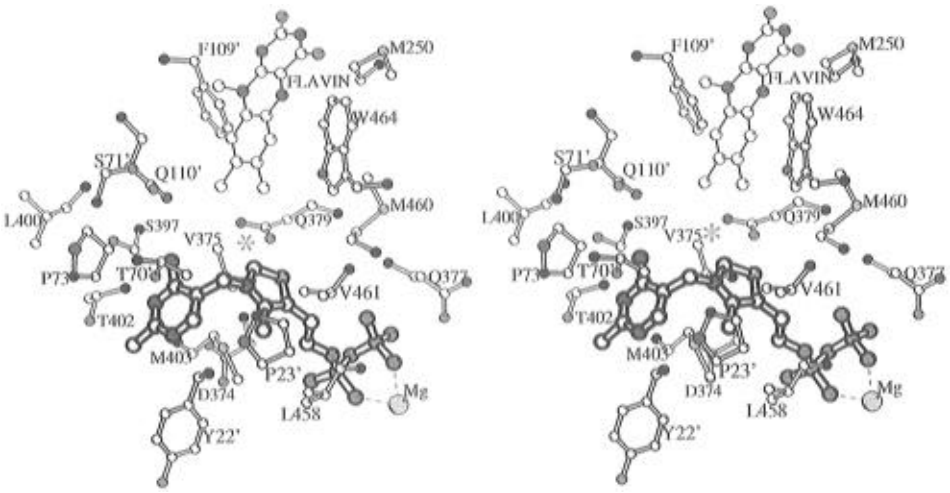

FIGURE 5: Proposed structure of the active site region of AHAS II. TPP, drawn in heavy lines, is shown with its pyrimidine to the left and its pyrophosphate bound to Mg^{2+} to the right. Substrate and product would enter and leave the active site from the top of the picture. Side chains and Cα atoms (black) are shown for residues within 7 Å of the position (marked by an asterisk) which would be occupied by the reactive carbanion of hydroxyethyl-TPP. For clarity, Gly residues are not shown. Residues labeled with a prime (′) belong to subunit B in the dimer, while unprimed residues belong to subunit A (see Figure 3). Heteroatoms of side chains and of the cofactors TPP and FAD are in gray, and carbon atoms other than Cα are unshaded.

at a few other positions in AHAS I are different from those in the enzymes of known high specificity, but none of the latter residues is near the substrate site in the model. These three residues were thus candidates for experimental examination of the active site by mutagenesis.

Site-Directed Mutagenesis. We tested whether any of these residues is important for substrate recognition, by mutagenesis of the amino acids at the equivalent positions (T70, M460, and W464) in isozyme II from *E. coli*, which is highly specific for reaction with α-ketobutyrate ($R = 65$). Nine enzymes with mutations at these positions have now been constructed, by the procedures described in Materials and Methods, and a number of their properties have been examined (Table 1).

Replacement of Trp464 leads to a decrease in the specificity, *R*, by 8−20-fold, even if another aromatic (Tyr or Phe) or aliphatic (Leu) residue is introduced in its place. The effect of these mutations on the stability of the enzyme or its affinity for FAD or TPP is relatively small, except for a 4−5-fold increase in K_M for TPP in W464 → A. This suggests that there is a direct interaction between Trp464 and the terminal methyl group of a reacting α-ketobutyrate molecule. The preference of an AHAS for the next higher homolog, α-ketovalerate, relative to pyruvate could also be determined in direct competition experiments like those used to determine *R* (Gollop et al., 1989) and supports an interaction of Trp464 with the second substrate. This nonphysiological specificity constant is about 1.9 for wild-

POX: *L. pla*	31	G I PG G	82	SA GP G	119	DT FQ E
POX: *E. col*		GV TG D		SC GP G		GY FQ E
AHAS: Eco-I	33	G I PG G	83	**C**S GP G	120	DA FQ E
AHAS: Eco-II	21	GY PG G	70	TS GP G	107	DA FQ E
AHAS: Eco-III	24	GY PG G	74	TS GP G	111	DA FQ E
AHAS: *S. cer*	112	GY PG G	162	TS GP G	199	DA FQ E
AHAS: *A. tha*		AY PG G		TS GP G		DA FQ E
AHAS: *N. tab*		AY PG G	166	TS GP G	203	DA FQ E
AHAS: *P. umb*		GY PG G		TS GP G		DA FQ E
AHAS: *B. fla*		G I PG G		TS GP G		DA FQ E
AHAS: *L. lac*		GY PG G		TS GP G		DA FQ E
GCL: *E. col*	24	GV PG A	75	TS GP A	112	ED FQ A
ALS: *K. pne*	31	G I PG A	80	TS GP G	117	QV HQ S
PDC: *Z. mob*	23	AV AG D	72	TY SV G	109	GH VL H

POX: *L. pla*	263	NR VA	393	DV GD I N	419	FA TM G	477	YG F I KD E
POX: *E. col*		GL I G		DV GT PT		HG SM A		LG FV AM E
AHAS: Eco-I	262	GM HG	390	DV GQ HQ	416	LG TM G	474	LG **L**V HQ **Q**
AHAS: Eco-II	249	GM HG	374	DV GQ HQ	400	LG TM G	458	LG MV RQ W
AHAS: Eco-III	259	GM HG	394	DV GQ HQ	420	LG SM G	478	LG MV KQ W
AHAS: *S. cer*	353	GM HG	496	GV GQ HQ	522	LG TM G	580	QG MV TQ W
AHAS: *A. tha*		GM HG		GV GQ HQ		LG AM G		LG MV MQ W
AHAS: *N. tab*		GM HG		GV GQ HQ		LG AM G	567	LG MV VQ W
AHAS: *P. umb*		GM HG		DV GQ HQ		LG TM G		QG MV RQ W
AHAS: *B. fla*		GM HG		GV GQ HQ		LG TM G		LG MV RQ W
AHAS: *L. lac*		GM HG		DV GQ HQ		MG TM G		LG MV RQ W
GCL: *E. col*	256	GL QT	392	T I GL SQ	418	AG PL G	476	LG L I RQ S
ALS: *K. pne*	260	VG LF	393	DM GS FH	419	QQ TM G	477	YN MV A I Q
PDC: *Z. mob*	262	WG EV	386	AE TG DS	412	WG HI G	470	YT I E VM I

FIGURE 6: Part of the alignment of the amino acid sequences of LpPOX (EC 1.2.3.3), some AHASs, and several related enzymes, in stretches in the region of LpPOX around the TPP-bound substrate. Amino acids corresponding to the consensus at a given position in AHASs are shown in bold type. Residues T70, L476, and Q480 in AHAS I are emphasized by underlining because they differ uniquely from the residues at the homologous positions in *all* other known wild-type AHASs (some 20 sequences from 14 organisms). The representative AHAS sequences shown are the catalytic subunits of three isozymes from *E. coli* (Friden et al., 1985; Lawther et al., 1981; Squires et al., 1983) and enzymes from the yeast *Saccharomyces cerevisiae* (Falco et al., 1985), higher plants *Arabidopsis thaliana* (Sathasivan et al., 1991) and *Nicotiana tobaccum* (Lee et al., 1988), alga *Porphyria umbilicalis* (Reith & Munholland, 1993), and bacteria *Brevibacterium flavum* (Inui et al., 1993) and *Lactococcus lactis* (Godon et al., 1992). The other enzymes are acetate-forming pyruvate oxidase (cytochrome) (POX, EC 1.2.2.2) from *E. coli* (Grabau & Cronan, 1986), glyoxylate carboligase (GCL, EC 4.1.1.47) from *E. coli* (Chang et al., 1993), catabolic (non-FAD-requiring) acetolactate synthase (ALS, EC 4.1.3.18) from *Klebsiella pneumonia* (Chang & Cronan, 1988), and pyruvate decarboxylase (PDC, EC 4.1.1.1) from *Zymomonas mobilis* (Conway et al., 1987). The sequence positions of the beginning of each stretch are indicated.

type AHAS II and is decreased to 0.16 and less than 0.1, respectively, in the mutants W464 → F and W464 → Q. Furthermore, the reverse mutation replacing the naturally occurring Gln in this position in AHAS I with Trp, Q480 → W (Yadav et al., 1986), *increases R* for α-ketobutyrate from 2.0 to 3.8. Since these experiments have not been carried out with purified enzyme, the amount of mutant protein, and hence relative activities of the mutants, can only be estimated (see Materials and Methods). However, it appears that mutation at Trp464 does not strongly affect the overall catalytic activity of AHAS II; *i.e.*, these mutants all seem to have activity within 1 order of magnitude of that of the wild-type enzyme.

In contrast with the effect of mutations at Trp464, mutation of Met460 in AHAS II has little effect on specificity for the second substrate (Table 1). However, replacement of this residue with a small (Ala), and particularly with a polar (Asn) amino acid, does markedly lower the stability of the protein and its affinity for its cofactors. Replacement of Thr70 with the residue found at the same position in AHAS I, Cys, also has little or no effect on the specificity.

On the basis of the effects of mutations at these positions, we can propose a model for the interaction of the substrates with the active site of AHAS. Figure 7 shows the TPP-bound acetohydroxybutyrate intermediate in the active site of AHAS II. The methyl derived from α-ketobutyrate (C4″) is in the region of Trp464, and we suggest on the basis of the mutagenesis data of Table 1 that the interaction between them contributes 1.3 kcal mol^{-1} [$=RT$ ln(65/8)] or more to the stabilization of the transition state for the product-determining step(s) of the reaction. The effect of this tryptophan probably includes van der Waals forces between the methyl group and the polarizable indole ring of the side chain, as well as possible alterations in the packing of neighboring residues. The Met460 side chain is packed between Trp464, the flavin, and other groups in a hydrophobic region and is not far from the thiazolium ring of TPP so that its replacement with, *e.g.*, Asn, would be unfavorable. The 4′-imino group on the pyrimidine of TPP, which has been proposed to play a role as a base in some TPP-dependent enzymes (Arjunan et al., 1996; Lindqvist et al., 1992; Muller et al., 1993), would be in a position to remove a proton from the hydroxyl at C1″, to assist elimination of the coenzyme from the product. The only side chain in a position to form polar interactions with the product carboxyl and hydroxyl groups attached to C2″ is apparently Gln110′ (from the neighboring subunit).

Mutagenesis of Trp464 has another significant effect (Table 1), a decrease of 1−2 orders of magnitude in the sensitivity of AHAS II to inhibition by the sulfonylurea herbicide sulfometuron methyl. It has already been observed that spontaneous mutations leading to sulfonylurea resistance arise at the Trp in this position in AHAS from yeast (Mazur & Falco, 1989) and higher plants (Bernasconi et al., 1995; Hattori et al., 1995; Lee et al., 1988). In our model, this residue is near the bottom of the funnel-shaped depression

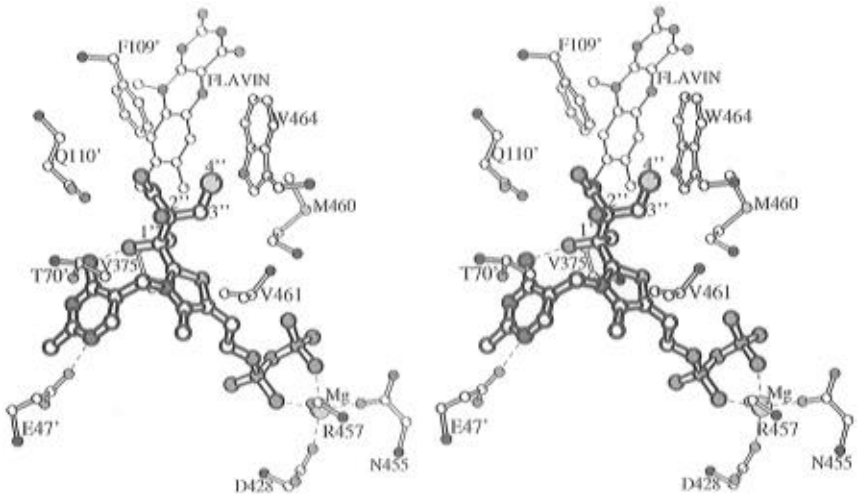

FIGURE 7: Interaction of the active site of AHAS II with substrates. TPP-bound acetohydroxybutyrate, which is the final intermediate in the reaction with α-ketobutyrate as the second substrate, is shown. The intermediate was constructed with the configuration at C1″ and the rotations around single bonds (C2−C1″, C1″−C2″, and C2″−C3″) chosen so as to bring the C4″ methyl of the product close to the Trp464 side chain and allow a hydrogen bond between an imino group on N4′ of the TPP pyrimidine and the hydroxyl at C1″ while minimizing steric interference and unsatisfactory dihedral angles. The rotations around the bonds connecting the thiazolium and pyrimidine moieties of TPP are slightly different from those in the LpPOX structure. The conserved Gln110′ is the only side chain capable of polar interactions with the carboxyl and the hydroxyl at C2″. Glu47′ polarizes the pyrimidine of the TPP. Asp428, Asn455, and the main chain carbonyl of Arg457 are ligands of the Mg^{2+}. Substrate and product would enter and leave the active site from the top of the picture.

Table 1: Catalytic Properties of Site-Directed Mutants of AHAS II[a]

construct	K_M, pyruvate (mM)	specificity for 2KB (*R*)[b]	K_i for SMM[c] (μM)	$t_{1/2}$ at 55 °C[d] (min)	K_M for TPP (μM)	K_M for FAD (μM)
wild type	5	65	<1	18	0.6	0.09
W464 → Y	3	7	~25	16	0.9	0.07
W464 → F	10	7	15	22	1.5	0.12
W464 → L	6	1.3	>20	17	0.4	0.16
W464 → Q	11	4	>20	10	0.7	0.12
W464 → A	4	8	>20	8	2.7	0.15
M460 → L	6	70	<1	25	2.4	0.14
M460 → A	9	22	8	8	7.6	0.6
M460 → N	6	53	>20	2	32	4.6
T70 → C	30	65	<1	1	2.0	0.1

[a] Mutants were constructed as described (Materials and Methods) and the mutated plasmids transduced into the AHAS$^-$ *E. coli* K12 strain BUM1 and grown under standard conditions for the expression of AHAS activity (Sella et al., 1993). Catalytic properties were determined by the standard method (Sella et al., 1993) at 37 °C and pH 7.6 in 0.1 M potassium phosphate buffer containing 40 mM pyruvate, 0.1 mM TPP, 25 μM FAD, and 10 mM $MgCl_2$, unless otherwise indicated. [b] The specificity ratio *R* was determined by following the simultaneous formation of acetohydroxybutyrate and acetolactate in the presence of varying concentrations of α-ketobutyrate and 40 mM pyruvate (Gollop et al., 1989). [c] The apparent K_i for the herbicide sulfometuron methyl (SMM) was estimated from the average rate over 20 min in the presence of 40 mM pyruvate and various concentrations of SMM; where K_i > 20 μM, this concentration of SMM led to a less than 10% decrease in activity. [d] The half-life for the loss of activity at 55 °C was estimated by preincubation of the enzyme for varied times in buffer containing 0.1 M FAD, 1 mM DTT, and 10 mM EDTA, followed by assay.

in the protein surface which allows access of substrates to the thiazolium ring. The binding of a sulfonylurea in this depression, in contact with the Trp, might block this access. Spontaneous mutations at a number of other positions (Bernasconi et al., 1995; Lee et al., 1988; Mazur & Falco, 1989; Yadav et al., 1986) have also been shown to lead to sulfonylurea resistance in one or another AHAS. An examination of the positions in the model structure, of the homologous residues of AHAS II, shows that they are all located at the surface of the access funnel (Figure 8), despite their wide separation along the linear sequence of the polypeptide. The model thus explains much of the experimental data on sulfonylurea resistance in AHAS and is consistent with observations and suggestions of Schloss and co-workers (Schloss & Aulabaugh, 1990; Schloss et al., 1988) concerning the "extrinsic" nature of the herbicide site.

Further Implications of the Model. A useful three-dimensional model for the active site of an enzyme should lead to further testable hypotheses about the mechanism of the enzyme. A number of them arise from the model we have presented. The model raises a question concerning the structure and possible function of the C terminus of AHAS II. In LpPOX (Muller & Schulz, 1993), about 60 residues (the last nine of which are disordered in the crystal structure) form a C-terminal minidomain which packs back on to the middle, FAD-binding domain. The C terminus of AHAS II is shorter by some 45 residues, and the structure of this 18-amino acid tail cannot be stable as drawn (Figure 3). One possible role for this C-terminal region would be to act as a flexible "flap" which could close off the active site, perhaps to prevent the hydroxyethyl-TPP carbanion from undergoing protonation or reaction with oxygen (Tse & Schloss, 1993). Many enzymes whose catalytic processes involve reactive species which must be protected from reactions with bulk solvent are thought to undergo conformational changes which close off the site upon substrate binding (Kepner, 1993; Lorimer et al., 1993; Pompliano et al., 1990), and C-terminal flaps fulfill this role in, *e.g.*, phosphoglyceromutases (Fothergill-Gilmore & Watson, 1989; Winn et al., 1981). A functional role for the C-terminal tail of AHASs is also suggested by the intriguing report of a mutation at residue 653 in *Arabidopsis* AHAS which leads to resistance to one of the imidazolinone herbicides (Sathasivan et al., 1990). Mutagenesis experiments under way in our laboratories suggest that removal of 12 amino acids from the C terminus of an AHAS catalytic subunit may be sufficient to strongly cripple its ability to synthesize acetolactate. Further examination of the role of the C terminus is certainly of importance.

Do the proposed interactions shown in Figure 7 suggest why the pyruvate oxidases carry out electron transfer from

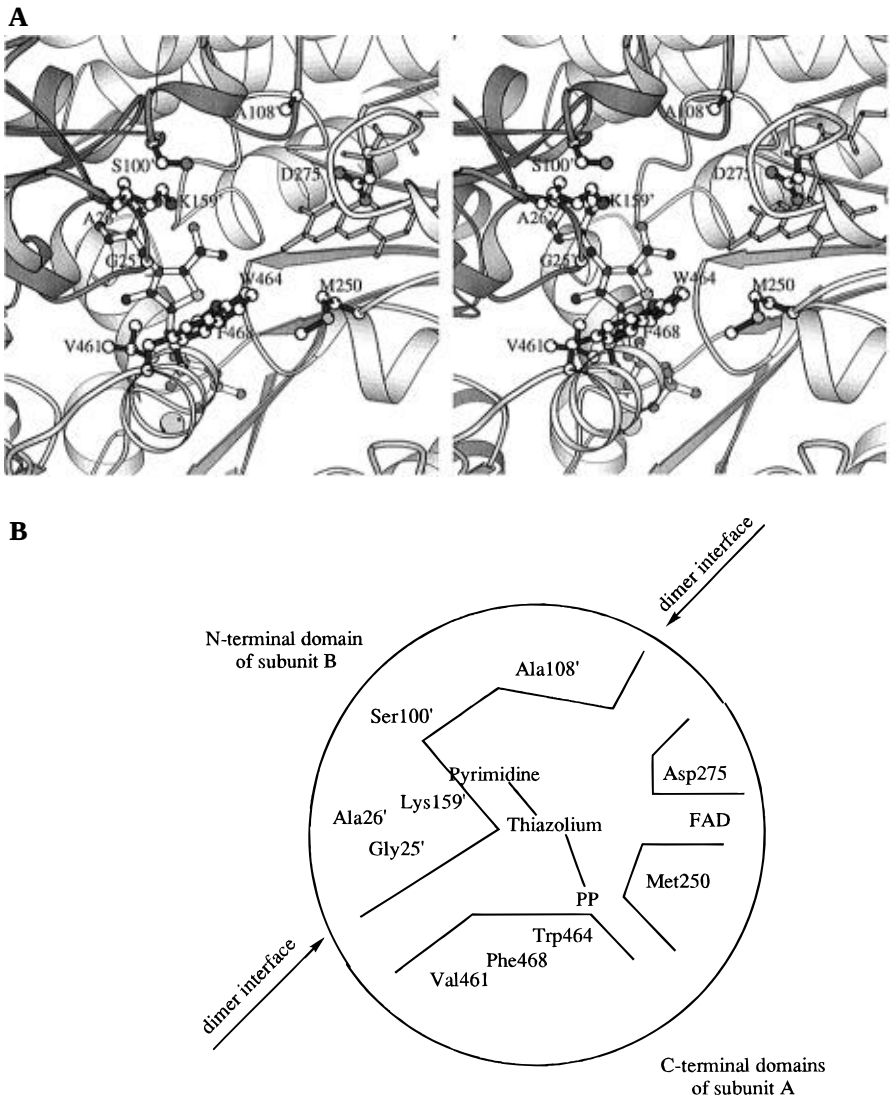

FIGURE 8: (A) Substrate access channel of AHAS II, looking down toward a hydroxyethyl-TPP intermediate (dark ball and light stick object) bound at the active site. The ribbons represent the main chains of two subunits; the C-terminal domain of subunit A (light) and the N-terminal domain of subunit B (dark) contribute to the site. The 10 labeled residues, whose side chains are shown as white ball and dark stick structures, are sites of (or homologous to sites of) spontaneous mutations conferring sulfonylurea resistance in one or another AHAS (see Discussion). (B) Cartoon representation of the active site depression.

the hydroxyethyl-TPP carbanion to the flavin, while AHASs [and the homologous (Chang et al., 1993) glyoxylate carboligase (GCL, EC 4.1.1.47), which presumably catalyzes the similar condensation of hydroxymethyl-TPP with glyoxylate] do not? Schulz and co-workers suggest (Muller & Schulz, 1993; Muller et al., 1994) that the benzene rings of Phe121′ or Phe479 (or both) of LpPOX might serve in the relay of electrons to the flavin. Since a Phe residue homologous to Phe121′ is conserved in all the AHASs and in GCL (Figure 6), it is unlikely that it *alone* is sufficient for the relay. Phe479 is replaced by nonaromatic hydrophobic groups (Leu and Met) in AHASs and GCL. Moreover, the two charged groups, Arg264 and Glu483, suggested (Muller & Schulz, 1993; Muller et al., 1994) to stabilize transient electron transfer to Phe479 in LpPOX, are replaced by hydrophobic or polar noncharged residues in these nonoxidative, FAD-dependent enzymes (*e.g.*, M250 and W464 in AHAS II; see Figure 6). The loss of the electron transfer pathway, and the concomitant formation of a binding pocket for a second α-keto acid, must lead to the condensation activities of AHAS and GCL; it is conceivable that the alteration of a handful of residues suffices to produce this functional change. Other suggestions arise from consideration of the homologies among these enzymes (Figure 6); it is tempting to suggest that in GCL the replacement of two valine residues flanking the thiazolium ring of TPP (*e.g.*, Val375 and -461 of AHAS II) by the larger isoleucine restricts the second substrate to glyoxylate (the α-keto acid with only two carbon atoms).

Conclusions. Construction of a model for the structure of the catalytic dimer of AHAS II, on the basis of its homology with LpPOX, leads to considerable insight into the function of the AHASs in general. The model suggests hypotheses for the roles of many portions of the protein in important functional properties of AHAS: coenzyme binding, catalysis of a specific reaction and avoidance of others, substrate specificity, and herbicide recognition. Many of these hypotheses should be testable by site-directed mutagenesis and careful analysis of multiple properties of the mutated proteins. The results of one such series of mutagenesis experiments, reported here, support a particular model for substrate recognition (Figure 7), in which a tryptophan residue (Trp464 in AHAS II) is an important factor in the preference for α-ketobutyrate. The combination

of homology modeling with site-directed mutagenesis and examination of multiple enzyme properties is clearly a powerful tool for the understanding of these enzymes.

ACKNOWLEDGMENT

We are grateful to Y. A. Muller and G. E. Schulz for making the preliminary coordinates for LpPOX available to us before release to the Brookhaven Protein Data Bank. Discussions with Dr. Dagmar Ringe, and the hospitality, advice, and assistance to D.M.C., by her research group and others at Brandeis University (particularly, Daniel Peisach, Ezra Peisach and Phil Xiang), were of inestimable value in the preparation of the manuscript. The capable technical assistance of N. Levy and M. Einav at Ben-Gurion University of the Negev is gratefully acknowledged. D.M.C. is the incumbent of the Lily and Sidney Oelbaum Chair in Applied Biochemistry.

REFERENCES

Arjunan, P., Umland, T., Dyda, F., Swaminathan, S., Furey, W., Sax, M., Farrenkopf, B., Gao, Y., Zhang, D., & Jordan, F. (1996) *J. Mol. Biol. 256*, 590−600.

Barak, Z., Chipman, D. M., & Gollop, N. (1987) *J. Bacteriol. 169*, 3750−3756.

Bernasconi, P., Woodworth, A. R., Rosen, B. A., Subramanian, M. V., & Siehl, D. L. (1995) *J. Biol. Chem. 270*, 17381−17385.

Bowie, J. U., Lüthy, R., & Eisenberg, D. (1991) *Science 253*, 164−170.

Breslow, R. (1958) *J. Am. Chem. Soc. 80*, 3719−3726.

Chang, Y.-Y., & Cronan, J. E., Jr. (1988) *J. Bacteriol. 170*, 3937−3945.

Chang, Y.-Y., Wang, A. Y., & Cronan, J. E., Jr. (1993) *J. Biol. Chem. 268*, 3911−3919.

Cohen-Fix, O., & Livneh, Z. (1992) *Proc. Natl. Acad. Sci. U.S.A. 89*, 3300−3304.

Conway, T., Osman, Y., Konnan, J., Hoffmann, E., & Ingram, L. O. (1987) *J. Bacteriol. 169*, 949−954.

Eoyang, L., & Silverman, P. M. (1986) *J. Bacteriol. 166*, 901−904.

Falco, S. C., Dumas, K. S., & Livak, K. J. (1985) *Nucleic Acids Res. 13*, 4011−4027.

Fothergill-Gilmore, L. A., & Watson, H. C. (1989) *Adv. Enzymol. Relat. Areas Mol. Biol. 62*, 227−313.

Friden, P., Donegan, J., Mullen, J., Tsui, P., Freundlich, M., Eoyang, L., Weber, R., & Silverman, P. M. (1985) *Nucleic Acids Res. 13*, 3979−3993.

Genetics Computer Group (1991) *Program manual for the GCG package*, Version 7, Genetics Computer Group, Madison, WI.

Godon, J.-J., Chopin, M.-C. M., & Ehrlich, D. S. (1992) *J. Bacteriol. 174*, 6580−6589.

Gollop, N., Damri, B., Barak, Z., & Chipman, D. M. (1989) *Biochemistry 28*, 6310−6317.

Gollop, N., Damri, B., Chipman, D. M., & Barak, Z. (1990) *J. Bacteriol. 172*, 3444−3449.

Grabau, C., & Cronan, J. E., Jr. (1986) *Nucleic Acids Res. 14*, 5449−5460.

Green, J. B. (1989) *FEBS Lett. 246*, 1−5.

Harms, E., Hsu, J. H., Subrahmanayam, C. S., & Umbarger, H. E. (1985) *J. Bacteriol. 164*, 207−216.

Hattori, J., Brown, D., Mourad, G., Labbe, H., Ouellet, T., Sunohara, G., Rutledge, R., King, J., & Miki, B. (1995) *Mol. Gen. Genet. 246*, 419−425.

Ho, S. N., Hunt, H. D., Horton, R. M., Pullen, J. K., & Pease, L. R. (1989) *Gene 77*, 51−59.

Inui, M., Vertes, A. A., Kobayashi, M., Kurusu, Y., & Yukawa, H. (1993) *DNA Sequence 3*, 303−310.

Jones, T. A. (1978) *J. Appl. Crystallogr. 11*, 268−272.

Jones, T. A., Zhou, J.-Y., & Cowan, S. W. (1991) *Acta Crystallogr. A47*, 110−119.

Kepner, E. S. (1993) *FEBS Lett. 326*, 4−10.

Kluger, R. (1987) *Chem. Rev. 87*, 863−876.

Kraulis, P. J. (1991) *J. Appl. Crystallogr. 24*, 946−950.

Lawther, R. P., Calhoun, D. H., Adams, C. W., Hauser, C. A., Gray, J., & Hatfield, G. W. (1981) *Proc. Natl. Acad. Sci. U.S.A. 78*, 922−925.

Lee, K. Y., Townsend, J., Tepperman, J., Black, M., Chui, C. F., Mazur, B., Dunsmuir, P., & Bedbrook, J. (1988) *EMBO J. 7*, 1241−1248.

Lindqvist, Y., Schneider, G., Ermler, U., & Sundstrom, M. (1992) *EMBO J. 11*, 2373−2379.

Lorimer, G. H., Chen, Y.-R., & Hartman, F. C. (1993) *Biochemistry 32*, 9018−9024.

Lu, M. F., & Umbarger, H. E. (1987) *J. Bacteriol. 169*, 600−604.

Mazur, B., & Falco, S. C. (1989) *Annu. Rev. Plant Physiol. 40*, 441−470.

Muller, Y. A., & Schulz, G. E. (1993) *Science 259*, 965−967.

Muller, Y. A., Lindqvist, Y., Furey, W., Schulz, G. E., Jordan, F., & Schneider, G. (1993) *Structure 1*, 95−103.

Muller, Y. A., Schumacher, G., Rudolph, R., & Schulz, G. E. (1994) *J. Mol. Biol. 237*, 315−335.

Pompliano, D. L., Peyman, A., & Knowles, J. R. (1990) *Biochemistry 29*, 3186−3194.

Reith, M., & Munholland, J. (1993) *Curr. Genet. 23*, 59−65.

Sambrook, J., Fritsch, E. F., & Maniatis, T. (1989) *Molecular cloning: a laboratory manual*, Cold Spring Harbor Laboratory Press, Plainview, NY.

Sathasivan, K., Haughn, G. W., & Murai, N. (1990) *Nucleic Acids Res. 18*, 2188.

Sathasivan, K., Haughn, G. W., & Murai, N. (1991) *Plant Physiol. 97*, 1044−1050.

Schloss, J. V., & Aulabaugh, A. (1990) in *Biosynthesis of Branched Chain Amino Acids* (Barak, Z., Chipman, D. M., & Schloss, J. V., Eds.) pp 329−356, VCH, Weinheim, Germany.

Schloss, J. V., Ciskanik, L. M., & VanDyk, D. E. (1988) *Nature 331*, 360−362.

Sella, C., Weinstock, O., Chipman, D. M., & Barak, Z. (1993) *J. Bacteriol. 175*, 5339−5343.

Squires, C. H., DeFelice, M., Devereux, J., & Calvo, J. M. (1983) *Nucleic Acids Res. 11*, 5299−5313.

Tse, J. M. T., & Schloss, J. V. (1993) *Biochemistry 32*, 10398−10403.

Umbarger, H. E. (1987) in *Escherichia coli and Salmonella typhimurium. Cellular and molecular biology* (Neidhardt, F. C., Ingraham, J. L., Low, B. L., Magasanik, B., Schaechter, M., & Umbarger, H. E., Eds.) pp 352−367, American Society for Microbiology, Washington, DC.

Vyazmensky, M., Sella, C., Barak, Z., & Chipman, D. M. (1996) *Biochemistry 35*, 10339−10346.

Weinstock, O., Sella, C., Chipman, D. M., & Barak, Z. (1992) *J. Bacteriol. 174*, 5560−5566.

Winn, S. I., Watson, H. C., Harkins, R. N., & Fothergill, L. A. (1981) *Philos. Trans. R. Soc. London B293*, 121−130.

Yadav, N., McDevitt, R., Benard, S., & Falco, S. C. (1986) *Proc. Natl. Acad. Sci. U.S.A. 83*, 4418−4422.

BI961588I